DETERMINATION OF THE POINT SPREAD FUNCTION OF YOHKOH SOFT X-RAY TELESCOPE

T. Sakurai and J. Shin

National Astronomical Observatory, 2-21-1 Osawa, Mitaka, Tokyo 181-8588, Japan

ABSTRACT

We re-evaluated the point spread function (PSF) of *Yohkoh* soft X-ray telescope. The best-fit model to the ground experimental data can be obtained by considering the undersampling effect at the central area of the PSF. Our result shows that the core of the Moffat function which models the PSF begins to be smoothly connected to the scattering wing at the distance of about $15''$ from the peak. Although the available experimental data are limited, the first-order vector perturbation theory helps us to consider the wavelength dependence of the scattering wing of the PSF. The autocovariance function of the SXT mirror surface roughness is expressed in our study by the product of exponential function and the modified Bessel function. The calculated angular distribution of the scattering component is compared satisfactorily with the result of in-flight data analysis. The results of the wavelength dependence of the PSF are discussed in detail.

INTRODUCTION

The Soft X-Ray Telescope (SXT) aboard *Yohkoh* has allowed us to study the details of three-dimensional structures of the solar corona since it was launched in 1991. However, according to the finite width of the point spread function (PSF) of the SXT mirror, it is expected that a certain amount of blurring effect, together with noise in the data, is inherent in the observed images. Thus it is necessary to subtract these components from the observed images in order to use those images for both morphological and photometric purposes. For a restoration of a true image from an observed SXT image, we need to know the detailed information on the shape of the PSF.

EXPERIMENTAL DATA OF THE PSF

Calibrations of the PSF of *Yohkoh* SXT mirror were carried out twice before the launch: One was at Marshall Space Flight Center (MSFC) (Tsuneta *et al.* 1991), and another was at White Sands Missile Range (WSMR) (Martens *et al.* 1995). Though both of these tests revealed the mirror to have excellent low-scatter and imaging properties, the detailed interpretation is quite different from each other. Figure 1 shows the comparison of the PSFs evaluated from the two ground experiments. It is clearly seen from the figure that the PSF from MSFC is much sharper than that from WSMR. It was demonstrated from the previous work (Shin 1988) that the deconvolution is very sensitive to the shape of the PSF, which means that this amount of deviation is not at all negligible.

Besides, the results of Martens *et al.* (1995) show large scatter. For the variation of the PSF as a function of the radial distance from the optical axis, the results of the two experiments show different patterns: For

MSFC, the full width at half maximum (FWHM) of the PSF changes from the center to the outermost part of the CCD. (Refer to Figure 4 in Tsuneta *et al.* (1991).) But for WSMR we cannot see any clear evidence of radial variation of the PSF. For the latter, it might be that a large scatter in WSMR data obstructed them to find the radial variation of the FWHM.

One more important point is that the reproducibility of the PSF for WSMR experiment was fairly low. They have obtained 6 different PSFs which were measured at the same X-ray beam locations on the CCD. Figure 2 shows the values of the coefficients a and b of the Moffat function $f(r) = c/\{1 + (r/a)^2\}^b$ obtained by Martens *et al.* (1995). We see that there is a large spread in the fitting coefficients of Moffat function. For instance, the FWHMs, which can be calculated using these coefficients, show the range of 3 to 5 arcsec. Under this situation, it is obvious that we are not able to determine the parameters at that location. We believe that this phenomenon is deeply related to the large scatter of the PSF obtained from WSMR experiment.

On the other hand, it is found from the figure that the coefficients a and b show a good linear relation. And this tells us that the large scatter of the coefficients might not only be due to noise in the data. If it is true, then it means that we should consider another factor for finding out a better fit to the PSF.

We believe the reason why Martens *et al.* (1995) could not reproduce the PSF properly is that they did not consider the undersampling effect at the peak of the PSF: It was revealed from the analyses of ground experiments (Tsuneta *et al.* 1991; Martens *et al.* 1995) that the FWHM of the PSF of *Yohkoh* SXT is only as large as 1 pixel size (2.45 arcsec) of the CCD. Since the SXT PSF has a very sharp peak and the pixel size is comparatively large, it is expected that the undersampling effect can change the shape of the peak of the PSF. Especially, though the location of the peak pixel is the same for a set of experiments, the actual center of the PSFs will be slightly different in a pixel from one experiment to another. In such a case, the sampling effect can produce different shapes of the peak at each PSF measurement.

For more precise determination of the PSFs, we have re-analyzed the WSMR data for six PSFs obtained at the same CCD location and evaluated the reproducibility. Figure 2 shows the comparison of the results of Martens *et al.* (1995) with ours. Though all the PSFs were obtained at the same location of the CCD pixel, their results show a wide range of coefficient values. On the other hand, after considering the undersampling effect, the range of deviation is much reduced in our results. We are now undertaking the re-analysis of the whole data sets of WSMR under the consideration of the undersampling effect. And we hope our work will be able to suggest a reasonable and better fit to the PSF of the *Yohkoh* SXT.

WAVELENGTH DEPENDENCE OF THE PSF

In general, the PSF of a telescope consists of two major components. One is the so-called geometrical component, which is due to the geometrical imperfectness, and does not have a wavelength dependence. The on-axis quality of an image is limited by the geometrical imperfections of the individual mirror shells and their alignment errors within the assembly. Another is the component due to the scattering on the mirror by the roughness of the mirror surface, which has a dependence on the wavelength. Thus only the scattering component will be different for different filters used in the observation of *Yohkoh* SXT.

The PSFs for different filters can be determined if the wavelength dependence of the scattering component was experimentally measured. However, for *Yohkoh* SXT, the evaluation of the scattering characteristics of the mirror was not performed prior to the launch. Only a limited amount of information can be deduced from in-flight data, such as accidental over-exposed flare images (Hara *et al.* 1994). In this study, we start from a basic theory of X-ray scattering by mirror surface and calculate the scattering intensity distribution and its wavelength dependence, and then compare the results with those obtained from the analysis of the over-exposed flare images. The latter is only available for a single filter (a single effective wavelength), but the theory allows us to extend the results to other wavelengths.

During the last two decades, extensive use of electromagnetic scattering theory has been made for the study of surface roughness by light scattering. First-order vector perturbation theory provides a means to estimate the influence of surface roughness on the imaging quality of the telescope (Church *et al.* 1977; de Korte *et al.* 1981). To estimate the influence of the surface roughness on the image quality, it is necessary that the surface should be described by a certain autocorrelation function. Several kinds of mathematical expressions, such as Gaussian or exponential, are possible for the description of the autocorrelation function. Recently Christensen *et al.* (1987) showed that an adoption of the modified Bessel function as an autocorrelation function evidently provided the best fit to the data for the X-ray telescopes on *ROSAT* and *EXOSAT*. Therefore it is chosen as the basic model correlation function here as well. A modification in our study is to introduce an exponential factor multiplied to the modified Bessel function, which suppresses the divergence of total scattering intensity for a particular r^{-2} dependence of the scattering characteristics of the SXT mirror.

The result of fitting of the theoretical scattering intensity distribution to the observed data is given in Figure 3. It is shown from this result that the level of the scattering component of the *Yohkoh* SXT mirror is comparatively low. For the wavelength of 8.3Å, the total intensity obtained from the integration on the whole CCD surface is about 11 %, which is very low compared to about 22 % of *EXOSAT* mirror (de Korte *et al.* 1981). The figure shows that the scattering component begins to be smoothly connected to the core of the PSF at the distance of about 6 pixels, which is equivalent to about 15 arcsec.

Figure 4 shows the wavelength dependence of the SXT PSF after the connection of the scattering wing to the core of the PSF is made. The wavelength dependence of the total scattered intensity is estimated from the scalar perturbation theory (Bennet and Porteus 1960). It is found that the shape of the PSF core shows little wavelength dependence, and only the level of the scattering wing responds sensitively to the variation of the wavelength. The peak value of the PSF changes with wavelength, because the PSF integrated from the core to the scattering wing has to give a fixed value. Even for the beryllium filter which has the highest scattering wing, the peak is reduced by less than 10 % compared to the thin aluminium filter. However, we have to point out that we restricted ourselves to make a conservative estimation for the scattering component. From trial calculations of image deconvolution using the obtained PSF, we tend to obtain higher contrast (lower level of diffuse background) in the beryllium filter images if we assume a larger level of scattering. When the wavelength considered becomes shorter, the scattering level becomes higher, and the scattering wing approaches the core portion. For a short wavelength as in the beryllium filter, the shape of the PSF core might be affected by the scattering component.

Turning to the experimental data, as a matter of fact Martens *et al.* (1995) did not find any systematic change of the FWHM with respect to the wavelength. However, this could be because they did not consider the undersampling effect at the core portion of the PSF. Along with the re-evaluation of the experimental data by correcting for the undersampling effect, we are trying to improve our present model for the PSF of *Yohkoh* SXT.

REFERENCES

Bennett, H. E. and Porteus, J. O 1960, *J. Op. Soc. Am*, **53**, 1394
Christensen, F. E., Hornstrup, A. and Schnopper, H. W. 1987, *SPIE*, **830**, 51
Church, E. L., Jenkinsin, H. A. and Zavada, J. M. 1977, *Opt. Eng.*, **16**, 360
Hara, H., Tsuneta, S., Acton, L. W., Bruner, M. E., Lemen, J. R. and Ogawara, Y. 1994, PASJ, **46**, 493
de Korte, P. A. J., Giralt, R., Coste, J. N., Ernu, C., Frindel, S., Flamand, J. and Contet, J. J. 1981, *Appl. Op.*, **20**, 1080
Martens, P. C., Acton, L. W. and Lemen, J. R. 1995, *Solar Phys.*, **157**, 141
Shin, J. 1998, PhD Thesis, National Astronomical Observatory of Japan
Tsuneta, S. and 12 co-authors 1991, *Solar Phys.*, 136, 37

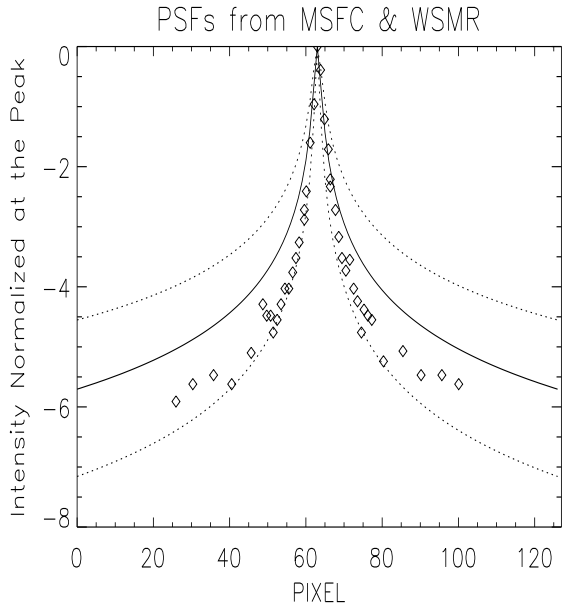

Figure 1

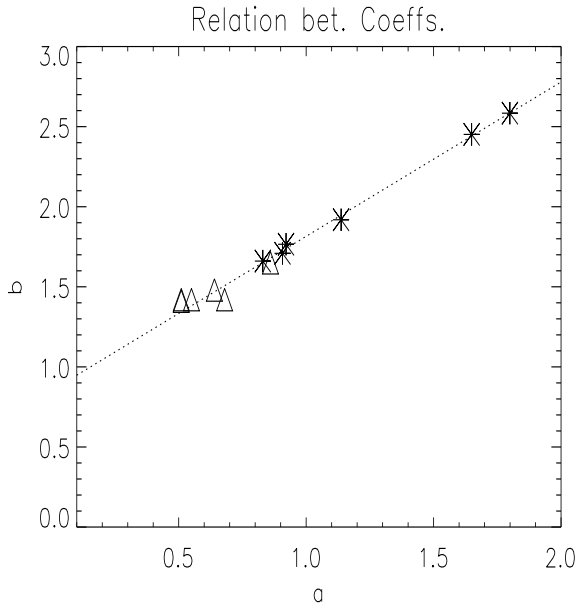

Figure 2

Figure 1: PSFs obtained from the ground experiments. Diamonds are the result from MSFC. Solid line is the result of WSMR. The dotted lines show the error range suggested by the measurement.

Figure 2: Relation between the coefficients a and b of Moffat function. Asterisks are for the results in Martens *et al.* (1995). Triangles are the results from our study.

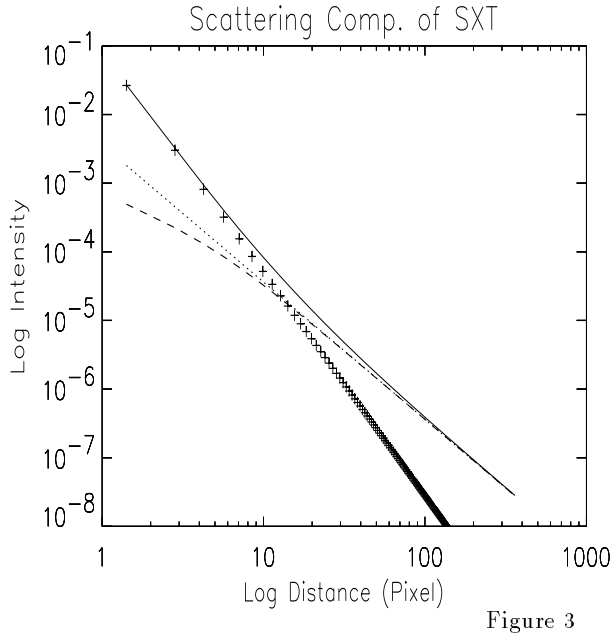

Figure 3

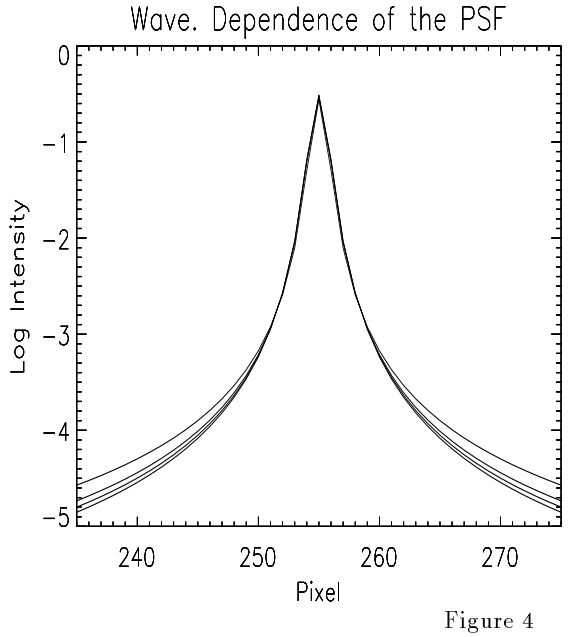

Figure 4

Figure 3: Estimation of the scattered intensity distribution of the thin Al filter of *Yohkoh* SXT (dashed line). The dotted-line is the power-law distribution of r^{-2}. Crossed marks are the extension of the Moffat distribution from the core. The solid line is the total feature of the SXT PSF obtained by the convolution of the Moffat function with the scattered intensity distribution.

Figure 4: Wavelength dependence of the scattered intensity distribution of the PSF of *Yohkoh* SXT (for thin Al, thick Al, 8.3 Å, and beryllium filter from the bottom to the top).